LANGMUIR Article
Cite This: Langmuir 2019, 35, 2412−2421
pubs.acs.org/Langmuir

Biomimetic Dextran-Based Hydrogel Layers for Cell Micropatterning over Large Areas Using the FluidFM BOT Technology

Andras Saftics,*[,†,‡] Barbara Türk,[†,‡] Attila Sulyok,[§] Norbert Nagy,[∥] Tamás Gerecsei,[†,⊥] Inna Szekacs,[†] Sándor Kurunczi,[†] and Robert Horvath[†]

[†]Nanobiosensorics Laboratory, Centre for Energy Research, [§]Thin Film Physics Department, Centre for Energy Research, and [∥]Photonics Department, Centre for Energy Research, Hungarian Academy of Sciences, Konkoly-Thege Miklós út 29-33, Budapest 1121, Hungary

[‡]Faculty of Chemical Technology and Biotechnology, Budapest University of Technology and Economics, Műegyetem rkp. 3, Budapest 1111, Hungary

[⊥]Department of Biological Physics, Eötvös Loránd University, Pázmány Péter stny. 1A, Budapest 1117, Hungary

Supporting Information

ABSTRACT: Micropatterning of living single cells and cell clusters over millimeter−centimeter scale areas is of high demand in the development of cell-based biosensors. Micropatterning methodologies require both a suitable biomimetic support and a printing technology. In this work, we present the micropatterning of living mammalian cells on carboxymethyl dextran (CMD) hydrogel layers using the FluidFM BOT technology. In contrast to the ultrathin (few nanometers thick in the dry state) CMD films generally used in label-free biosensor applications, we developed CMD layers with thicknesses of several tens of nanometers in order to provide support for the controlled adhesion of living cells. The fabrication method and detailed characterization of the CMD layers are also described. The antifouling ability of the CMD surfaces is demonstrated by in situ optical waveguide lightmode spectroscopy measurements using serum modeling proteins with different electrostatic properties and molecular weights. Cell micropatterning on the CMD surface was obtained by printing cell adhesion mediating cRGDfK peptide molecules (cyclo(Arg-Gly-Asp-D-Phe-Lys)) directly from aqueous solution using microchanneled cantilevers with subsequent incubation of the printed surfaces in the living cell culture. Uniquely, we present cell patterns with different geometries (spot, line, and grid arrays) covering both micrometer and millimeter−centimeter scale areas. The adhered patterns were analyzed by phase contrast microscopy and the adhesion process on the patterns was real-time monitored by digital holographic microscopy, enabling to quantify the survival and migration of cells on the printed cRGDfK arrays.

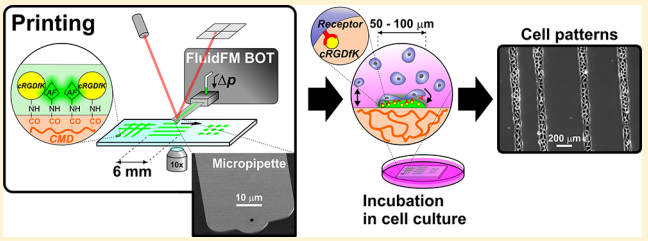

1. INTRODUCTION

Selective arrangement of biomolecules and cells on surfaces is of high interest in fundamental cell research, tissue engineering as well as biosensors using individual cells, cell clusters, or tissues for sensing.[1,2] Cell micropatterning can be used to perform high-throughput biological studies. In cell micropatterning strategies, the support surface to be patterned must fulfill several chemical and physical criteria.[3] The surface should be endowed with adhesion triggering biomolecules, and, at the same time, it should provide cell-repellent (antifouling) background, enabling to distinguish the patterned and nonpatterned areas.[4] In addition, for the long-term survival of cells (e.g., for investigating proliferation), the mechanical characteristic of the support must also be optimized (extracellular matrix, ECM-like stiffness). Hydrogel-based biomimetic coatings are very promising in fulfilling all of the above requirements.[5] Hydrogels are cross-linked hydrophilic polymer networks presenting large water uptake. Owing to their three-dimensional (3D) structure that provides enhanced internal surface and a great number of available conjugation sites, hydrogels can be functionalized by a much larger amount of biomolecules (e.g., bioreceptors) compared to the commonly used flatlike self-assembled monolayers. Moreover, hydrogels can provide a microenvironment bearing such chemical, hydration, and mechanical properties, which are close to the natural microenvironment of biomolecules and cells. Although hydrogels are widely used in tissue engineering as a culturing medium or in the field of biosensors as coatings for biomolecule detection,[6] the development of hydrogel layers suitable for combined applications, such as supporting the detection of cellular behavior on biosensor surfaces, is still strongly in demand. Main challenges in the development of these coatings are the stabilization of a relatively thick (10−1000 nm) layer with well-controlled thickness in order to

Received: September 25, 2018
Revised: January 14, 2019
Published: January 17, 2019

DOI: 10.1021/acs.langmuir.8b03249
Langmuir 2019, 35, 2412−2421

provide a proper mechanical support for cells by retaining the ability of sensing. Hydrogel layers prepared from the carbohydrate dextran or its commonly used derivative carboxymethyl dextran (CMD) are promising candidates, owing to their great protein- and cell-repellent abilities proven by a wide range of biosensor applications,[6] easy conjugability as well as biomimetic, ECM-like properties.[6−9] Our experiences show, however, a substantial difficulty in dextran layer preparation when aiming larger thickness in optical quality for biosensing.[10−12]

The most common method to endow hydrogels or other substrates with cell-adhesive abilities is the chemical modification with the Arg-Gly-Asp (RGD) tripeptide sequence, which is the minimal molecular sequence required by the integrin receptors for the recognition and subsequently initiated cell adhesion.[13] It was previously demonstrated that strongly cell-repellent carbohydrate surfaces can be selectively transformed to highly cell-adhesive by conjugating with RGD motifs.[14−18] Regarding the main peptide design principles, cyclization is applied to enhance conformational stability; moreover, the incorporation of flanking sequences can maximize the affinity and selectivity for the target integrins. The synthesis of the commonly used cyclic pentapeptide cRGDfK (cyclo(Arg-Gly-Asp-D-Phe-Lys)) is also based on the cyclization of linear RGD that is complemented with a D-phenylalanine (D-Phe) unit.[19,20]

Available methods for the micropatterning of hydrogel layers with cell-adhesive biomolecules are photolithography, stencil patterning, microfluidic patterning, microcontact printing, inkjet printing, as well as selective plasma etching.[1,21−23] However, among the micropatterning strategies, only few can provide fast pattern deposition with high resolution (e.g., arrays of single cells) and the ability to cover macroscopic areas at the same time. Photolithography, usually requiring precisely fabricated masks, has been shown to be an effective technique for patterning microarrays of cell-adhesive biomolecules such as RGD motifs over millimeter-scale areas of poly(ethylene glycol)-based surfaces.[24,25] The atomic force microscopy (AFM)-based micropipette technique (FluidFM BOT) is another straightforward method, which enables the printing of biomolecules directly from the liquid environment, providing a well-controlled, mask-free patterning of cells with a reduced number of fabrication steps and without the need for cleanroom conditions.

Nanolithography of biomolecules and nanoparticles directly from the liquid environment and manipulation of single cells have been major challenges to the traditional AFM-based techniques (such as dip-pen nanolithography). Printing micrometer-scale pattern elements over millimeter-scale surface areas is also very limited by these methods (the printed area typically ranges in the 1−100 μm scale).[26] FluidFM (fluidic force microscope) is a unique micromechanical and microfluidic device that combines the force-controlled high spatial precision of AFM with the capability of direct liquid delivery by microfluidics.[27] The technology can be used for printing two-dimensional surface patterns with various formations[28] or even for precisely controlled template-free 3D micro- and nanoprinting.[29,30] FluidFM enables the printing of micro-scale patterns on large, several millimeter−centimeter-sized areas directly from the aqueous solution of biomolecules intended to be printed. This feature, supplemented with the possibility of measuring adhesion forces or injecting other biomolecules or drugs into cells, is pivotal in the field of single-cell analysis and manipulation. Nowadays, novel techniques employ plate-based layouts, facilitating high-throughput screening. So far, only few papers deal with the printing of surface patterns of biomolecules using the FluidFM system (a relevant example is the nanoscale dispensing of streptavidin on biotin-functionalized surfaces[31]).

The main goal of this research is the development of a suitable hydrogel layer and micropatterning methodology for future applications of cell arrays deposited on waveguide-based optical biosensor surfaces. Here, we present a new type of CMD hydrogel layers developed for controlled cell-adhesion studies on micropatterned surfaces. The covalently bound CMD hydrogel layers were spin-coated onto microscope glass slides, and the CMD chains were cross-linked with sodium trimethaphosphate (STMP). The layers were characterized by various surface analytical methods [spectroscopic ellipsometry (SE), X-ray photoelectron spectroscopy (XPS), AFM, as well as contact angle (CA) measurements]. Because the cell-repellent ability of the coatings can be basically derived from a resistance to protein adsorption, we examined the adsorption of serum proteins [nonspecific binding (NSB)] on the CMD surface using a label-free biosensor technique, optical waveguide lightmode spectroscopy (OWLS). We present our methodology using the FluidFM BOT technique for micropatterning living cells on the developed CMD hydrogel surfaces. In the printing procedure, aqueous solution of cRGDfK molecules was printed onto the CMD surface and the patterned samples were incubated with HeLa cell culture. We applied digital holographic microscopy (DHM) for real-time monitoring the pattern-mediating adhesion and migration process. The concept of cell micropatterning can be seen in Figure 1.

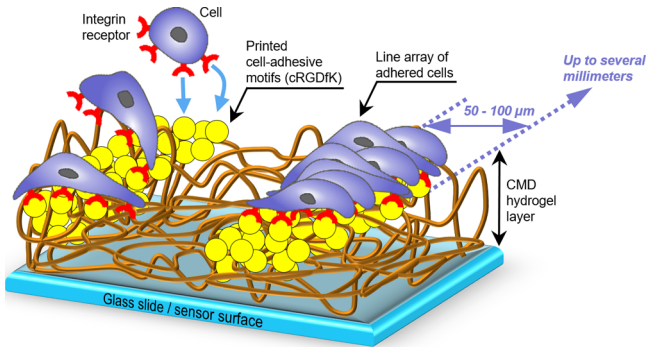

Figure 1. Cell adhesion to micropatterns of cell-adhesive motifs printed on the CMD-based hydrogel layer.

2. EXPERIMENTAL SECTION

2.1. Chemicals. Chromosulfuric acid used for substrate cleaning was obtained from VWR (Budapest, Hungary). Dextran T-500 (with 500 kDa molecular weight) was obtained from Pharmacosmos A/S, (Holbaek, Denmark). 3-Aminopropyltriethoxysilane (hereafter aminosilane), ethyl-3-(3-dimethylaminopropyl)-carbodiimide hydrochloride (EDC), and *N*-hydroxysuccinimide (NHS) as well as phosphate-buffered saline (PBS) were obtained from Sigma (Budapest, Hungary). Monochloroacetic acid employed for CMD synthesis was purchased from Thermo Fisher (Budapest, Hungary). Sodium hydroxide (NaOH) and STMP were purchased from VWR. Proteins, including bovine serum albumin (BSA), fibrinogen (FGN), and lysozyme (LYZ), were obtained in lyophilized form from Sigma (Budapest, Hungary). The reagents used for FluidFM printing experiments, including cRGDfK and 6-aminofluorescein (AF), were

DOI: 10.1021/acs.langmuir.8b03249
Langmuir 2019, 35, 2412−2421

obtained from GeneCust (Luxembourg) and Setareh Biotech (Eugene, USA), respectively. Regarding the solutions used for cell culture maintenance, Dulbecco's modified Eagle's medium (DMEM), L-glutamine, penicillin–streptomycin solution, trypsin-ethylenediaminetetraacetic acid solution, as well as paraformaldehyde were all purchased from Sigma (Budapest, Hungary). Fetal bovine serum was purchased from Biowest SAS (Nuaillé, France). Ultrapure grade water with a resistivity of 18 MΩ·cm was used. All chemicals and reagents were of analytical grade.

2.2. Fabrication of CMD Layers. *2.2.1. Preparation of Substrate Surfaces.* Concentrated chromosulfuric acid was used for cleaning the OWLS sensor chips and OWLS model surfaces (3 min), and it was followed by intensive rinse with ultrapure water and blowing with nitrogen stream.

The aminosilylation of cleaned substrates was performed in a heated vacuum chamber (Glass Oven B-585, BÜCHI Labortechnik AG, Flawil, Switzerland). The aminated surfaces were stored in a vacuum desiccator until use.

2.2.2. CMD Grafting. The developed CMD grafting method can be followed in Figure 2. Lyophilized CMD (synthetized using our

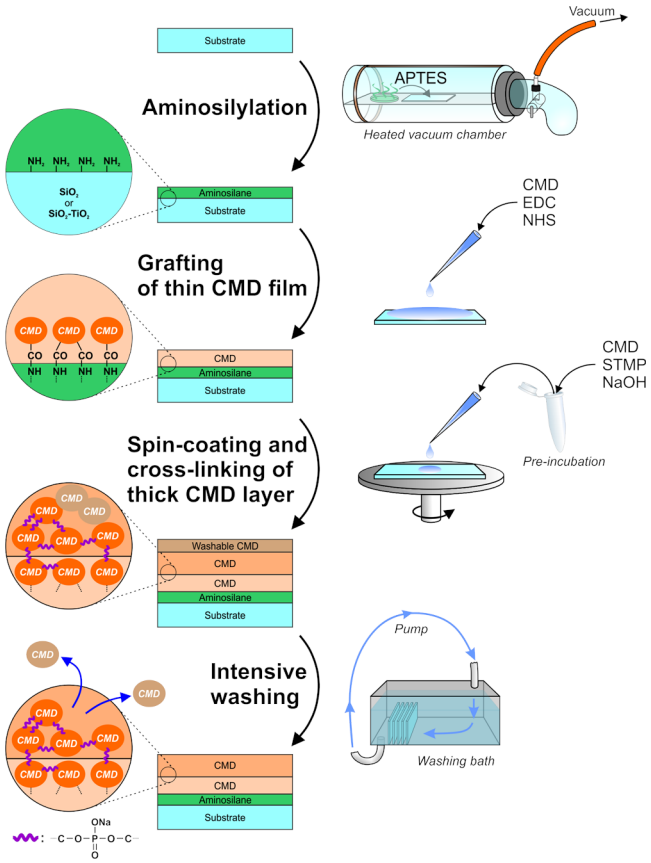

Figure 2. Fabrication of spin-coated and cross-linked CMD layers.

previously introduced method[10,32], degree of substitution: 0.145, molecular weight: 500 kDa) was dissolved in ultrapure water (concentration: 50 mg/ml), and the pH was neutralized using NaOH solution. The EDC and NHS reagents were dissolved in ultrapure water (0.4 M), and the aqueous solutions were added to the CMD solution. The following concentration ratios were used in the prepared CMD/EDC/NHS grafting solution: [COOH]/[EDC]/[NHS] = 6:1:1. Each of the aminosilylated substrates was incubated overnight with CMD/EDC/NHS solution at 4 °C. Then the surfaces were rinsed with ultrapure water and dried under nitrogen flow.

In the subsequent step, a CMD solution containing the STMP cross-linking agent was spin-coated onto the sample surfaces using various rotation speeds (1000, 2000, 4000, and 6000 rpm). The reagent concentrations in the spin-coated solution were as follows: 20 mg/mL CMD, 125 mM NaOH, and 50 mM STMP. STMP is reactive only with the carbohydrate hydroxyl groups, which is useful for retaining the functionality for receptor immobilization or other kind of conjugations. STMP cross-links carbohydrates by a phosphorylation reaction under alkalic conditions.[33−35]

After spin-coating, the samples were intensively washed in a Teflon tank. Ultrapure water and 0.1 M HCl were circulated using a large-scale peristaltic pump. The subsequent washing phases were as follows: ultrapure water (20 min), 0.1 M HCl (10 min), and ultrapure water (10 min). The procedure ended by drying the surfaces under nitrogen flow.

Besides the spin-coated CMD layers, ultrathin CMD films were also prepared for NSB experiments. The application of the ultrathin CMD layers in NSB experiments is presented in this work as new results. Further details of the related fabrication method and layer characterization can be found in our previous publication.[10]

2.3. Analytical Techniques. *2.3.1. Optical Waveguide Lightmode Spectroscopy.* We used the OWLS technique to measure the adsorption kinetics of selected proteins on CMD layers in order to quantify the layers' protein-repellent ability. The in situ OWLS measurements were performed by an ASI BIOS-1 instrument using type 2400 μV sensor chips (MicroVacuum Ltd., Budapest, Hungary). The transverse electric (TE) and transverse magnetic (TM) zeroth-order waveguide modes were excited by a He–Ne laser beam (632.8 nm) coupled into the chip's waveguide film. A precision goniometer was used to scan the coupling angles in every 14 s. The effective refractive indices (N_{TE}, N_{TM}) and surface mass density were measured with a sensitivity of 1×10^{-6} refractive index unit and 1 ng/cm^2, respectively. In separate refractive index measurements, the refractive index of PBS (n_{PBS}) and refractive index increment of protein solutions (dn/dc) were determined using a precision refractometer (632.8 nm, 25 °C; J157 automatic refractometer, Rudolph Research Analytical, Hackettstown, USA). The collected effective refractive index data were evaluated by the isotropic homogeneous four-layer mode equations. The following data were used in the evaluation: n_{PBS} = 1.3330, $dn/dc_{protein}$ = 0.1849 mL/g.

2.3.2. X-ray Photoelectron Spectroscopy. The cross-linking degree of CMD layers could be estimated by determining their elemental composition using XPS measurements. The XPS instrument is based on an X-ray source and photoelectron detector providing an energy resolution of 1.5 eV. During the measurements, ultrahigh vacuum was maintained (2×10^{-9} mbar). The following lines of main components were detected: Si $2p_{3/2}$ (100 and 103 eV for basic and oxide states, respectively), P 2s (189 eV), C 1s (at around 285–289 eV binding energies), N 1s (401 eV), Ti $2p_{3/2}$ (454 eV), Na Auger (497 eV), and O 1s (531 eV). The evaluation was performed using Shirley background subtraction as well as Gaussian/Lorentzian fitting.

2.3.3. Spectroscopic Ellipsometry. The thickness of the CMD layers spin-coated at varying rotational speeds was measured by the SE technique. The ellipsometric spectra were recorded on a Woollam M-2000DI rotating compensator spectroscopic ellipsometer (J.A. Woollam Co., Inc., Lincoln, USA). A microfocusing equipment was used to focus the source light to a 150 μm diameter spot area. The measurements were performed at 70° incident angle with a data acquisition time of 5 s, and the recorded spectra were obtained in the wavelength range of 191–1689 nm. Regarding the mapping measurements, a rectangular area of 12 mm × 8 mm was scanned using 3 and 2 mm grid distances in the x and y directions, respectively. The data were collected and evaluated using the CompleteEASE software (J.A. Woollam Co., Inc.).

2.3.4. Atomic Force Microscopy. The roughness of the CMD surfaces was characterized by AFM. A FlexAFM instrument (Nanosurf GmbH, Liestal, Switzerland) equipped with Tap 190GD-G type probes (BudgetSensors Ltd., Sofia, Bulgaria) was used to obtain AFM images about the CMD samples. Tapping mode scans were performed to obtain surface topographic images. The collected raw images were then analyzed by the Gwyddion software.

2.3.5. Contact Angle Measurements. Routine sessile drop measurements were applied to characterize the wetting and swelling

DOI: 10.1021/acs.langmuir.8b03249
Langmuir 2019, 35, 2412−2421

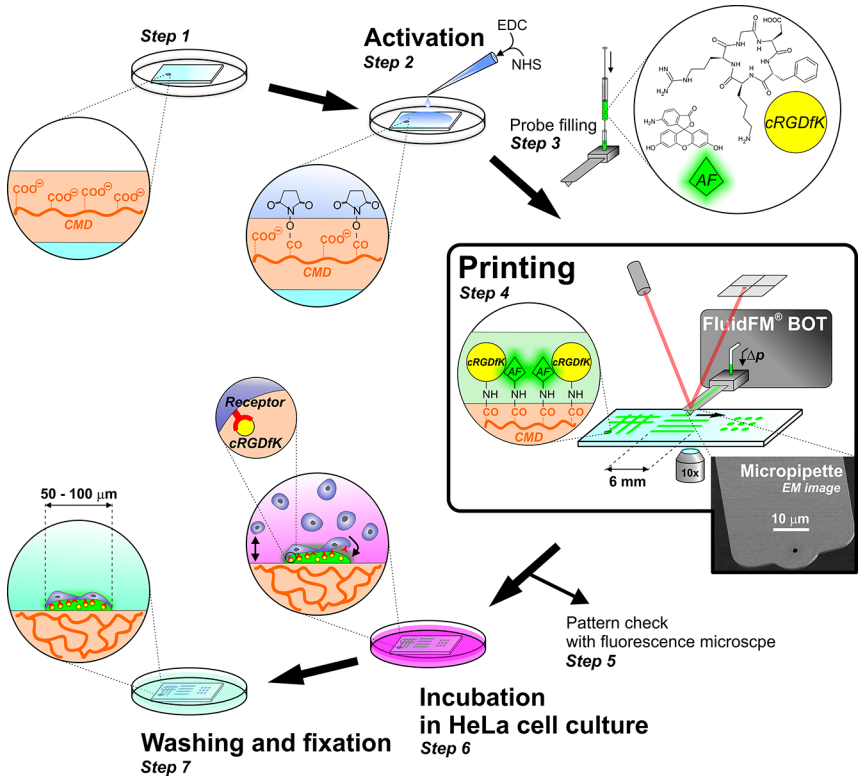

Figure 3. Method used for cell adhesion experiments on the cRGDfK-printed CMD surface, where microprinting was performed with the FluidFM technique (source of micropipette's electron microscopy image: courtesy from Cytosurge AG).

properties of the CMD layers. The hydrophilic nature and, as a result, the wetting behavior of the CMD layers have several effects on the applications: it has an important role in determining the protein- and cell-repellent abilities as well as the mechanical properties of the cell-adhesive support. Also, the wetting characteristics have a strong effect on the resulting prints including the resolution of the patterns. By detecting the layer's swelling behavior, the performed CA measurements could be used to prove the hydrogel nature of the CMD coating.

The measurements were conducted at room temperature by depositing drops with volumes of ca. 3 μL on the surface and increasing their volume up to ca. 5 μL. In the closed chamber with nearly saturated atmosphere, the drops were left for ca. 120 s to stabilize before capturing images. The CAs were calculated using the DropSnake software,[36] and the mean values of the left and right CAs for all samples were given.

The spreading dynamics measurements were performed using another setup equipped with a closed sample chamber with the following maintained conditions: T = 23 ± 0.5 °C, relative humidity: 89 ± 2%. One sample was inserted into the chamber, and the measurement was carried out immediately. A ca. 3 μL droplet was deposited onto the surface, and its spreading was followed and captured with a time resolution of 2 s. The captured images were analyzed by the Krüss DSA software using elliptic fit.

2.3.6. FluidFM BOT. Microlithography experiments were performed by a specially designed AFM-based instrument, the FluidFM BOT setup manufactured by Cytosurge AG (Glattbrugg, Switzerland). In this setup, the probe is a microchanneled (hollow) cantilever that is connected to a pressure controller via a fluidic circuit. The continuous and closed fluidic channel can be filled with a chosen solution. The pressure applied on the internal solution can eject the soluble molecules through the aperture that is located at the end of the cantilever. While the solution is ejected, the contact of the probe to the surface is continuously regulated by the force feedback established by a laser detection system of conventional AFM setups.[27,28,37] Under overpressure, the probe acts as a force-controlled micropipette, which enables to dispense droplets of solutions with down to a volume of 0.5 fL.[37]

The whole FluidFM BOT system involved an inverted optical microscope (Zeiss Axio Observer.Z1, Carl Zeiss AG, Oberkochen, Germany), a sample stage (x,y-stage) combined with an automated measurement head (z-stage) and mounted on the microscope, as well as the related controllers, including a pressure controller. Silicon nitride micropipettes manufactured by Cytosurge AG were used with 2 μm aperture size and 2 N/m stiffness (force constant). The probe was mounted in the head, and from that point, the whole process was operated via the ARYA software.

2.3.7. Phase Contrast and Fluorescent Microscopy. The cRGDfK−AF patterns as well as the adhered cell arrays were observed using fluorescent and phase contrast microscopy. Phase contrast images were captured using a Zeiss Observer.Z1 microscope (Carl Zeiss AG, Oberkochen, Germany) in bright-field mode. Fluorescent microscope images were also recorded by this instrument in the fluorescent mode. For capturing and image analysis, the AxioVision software (Carl Zeiss AG, Oberkochen, Germany) was used.

2.3.8. Digital Holographic Microscopy. DHM was used to real-time monitor the adhesion of HeLa cells. Real-time holographic images were recorded by a HoloMonitor M4 instrument (Phase Holographic Imaging PHI AB, Lund, Sweden). The captured images were analyzed and formatted using the HoloStudio M4 software (Phase Holographic Imaging PHI AB).

2.4. Experiments on the Fabricated CMD Layers. *2.4.1. NSB Experiments.* The protein-repellent ability of the fabricated CMD layers was tested using three different protein molecules with varying molecular weight and isoelectric point (pI) values. The applied proteins were BSA (66.5 kDa, pI = 4.7−5.1), FGN (340 kDa, pI = 5.5−6.0), and LYZ (14.3 kDa, pI = 11.0). The adsorbed protein mass was measured by the in situ OWLS method.

As a first experimental step, the sensor surface was conditioned with PBS (baseline), and then a flow of BSA dissolved in PBS at a concentration of 2 mg/mL was applied (30 min, 1 μL/s flow rate; adsorption phase). Finally, PBS flow was applied again until reaching

DOI: 10.1021/acs.langmuir.8b03249
Langmuir 2019, 35, 2412−2421

a stable signal (washing). The described phases were consecutively applied with 2 mg/mL solutions of FGN and LYZ, respectively.

2.4.2. Microlithography by the FluidFM BOT Technology. The methodology of sample preparation and FluidFM printing combined with cell adhesion experiments is illustrated in Figure 3. As a first step of the experiment, the carboxylic groups of the CMD layer prepared on the glass slide (Figure 3, step 1) were activated by EDC and NHS reagents (step 2). The aqueous solution of the reagents (0.2 M EDC, 0.2 M NHS) was pipetted on the center of the surface, and the drop was incubated for 30 min at room temperature. Followed by a rinse with ultrapure water, the surface was gently blown with nitrogen stream, and the sample was immediately mounted in the *x*,*y*-stage of the FluidFM BOT.

The reservoir of the FluidFM micropipette was filled using a Hamilton syringe with an aqueous phosphate buffered solution of 10 mg/mL cRGDfK and 0.5 mM AF (step 3). The solution was then driven into the microchannel of the cantilever by an applied pressure of 1000 mbar. The printing started with moving the probe over the surface (*z*-movement) and reaching a setpoint of 15 mV. A set of parameters used for the printing process are detailed in the Supporting Information. Three types of patterns were printed, including spots positioned as grid points (i), parallel lines ("line array", ii) as well as another line pattern, forming a grid (iii) (step 4). As the AF-containing prints were fluorescently active, each pattern could be checked by the fluorescent microscope and the results of printing could be rapidly assessed (step 5). The method also allowed to precisely determine the pattern positions. Afterward, the samples were sliced, and the slide pieces were put in a six-well plate (illustrated by just a simple Petri dish in Figure 3) for the subsequent cell adhesion experiments.

2.4.3. Cell Adhesion Experiments. For preconditioning of sample surfaces, 2.5 mL of cell-free DMEM was added to each well of a six-well plate prior to cell seeding. Meanwhile, HeLa cells were harvested, and cell suspension (250 μL, 2.5 × 10^6 mL^{-1}) was added to each well (for the cell maintenance protocol, see the Supporting Information). Followed by sedimentation (ca. 10 min), the plate containing the samples and added HeLa cells was moved into a humidified incubator (Figure 3, step 6). After 1 h of incubation, the floating cells were washed off. The samples were checked under the phase contrast microscope to assess the actual phase of the cell adhesion process. Afterward, additional 2−4 h incubation was applied in order to complete the adhesion. As a final step, the samples were washed with PBS, and the cells were fixed using paraformaldehyde solution (step 7). The fixed cell patterns were examined by phase contrast microscopy, and microscope images were recorded using 5×, 10×, and 40× objective lenses.

In separate cell adhesion experiments, the adhesion process was real-time monitored by DHM (HoloMonitor M4) according to our previously developed in situ setup.[38] Briefly, a rubber O-ring was placed on a selected area of the printed sample, and 140 μL of HeLa cell suspension containing 1.4 × 10^4 cells was pipetted into the inside area surrounded by the O-ring. A cover glass slide was placed on top of the O-ring, and the sample was positioned in the focus of the holographic microscope. 3D structures of cells were visualized by sample illumination with 0.1 mW/cm^2 He−Ne laser (635 nm). The interference pattern was recorded as a hologram on a digital sensor. The images were captured in every 5 min inside a humidified incubator.

3. RESULTS AND DISCUSSION

3.1. Characterization of CMD Layers. *3.1.1. Thickness, Cross-Linking Degree, and Wetting Behavior.* The CMD layers were prepared using various spin-coating rotational speeds to control their thickness. We developed an ellipsometric optical model in order to evaluate the obtained Ψ and Δ spectra and determine the thickness of dry CMD layers. The optical model and its applications in the characterization of spin-coated CMD layers (measurement of optical properties and thickness) can be found in our previous paper.[12]

CMD thickness values resulting from the ellipsometric evaluation are shown in Figure 4, representing both the deposited (unwashed) CMD layer and the remaining (washed) layer, prepared at different spin-coating rotational speeds. The rotational speed significantly affected the CMD layer thickness with decreasing thickness tendency as the rotational speed was increasing (as expected), and it was found that the thickness could be controlled in the range of 100−200 nm. However, washing the layers considerably decreased the thickness (thickness loss of ca. 80%), and the thickness of the resulting (remaining) layers was found to be in the range of 10−50 nm.

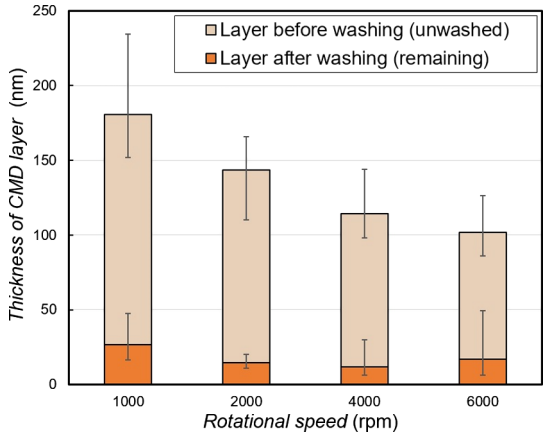

Figure 4. CMD layer thickness as a function of applied spin-coating rotational speeds. The height values of the top (light orange) columns represent the thickness of CMD layers as prepared. The height values of the bottom (dark orange) columns correspond to the thickness of the remaining layers. Each top value was averaged from data collected on three parallel samples and at the nine middle positions of each sample. The minimum and maximum thickness values are indicated by the given error bars.

The AFM measurements revealed that the surface of both washed and unwashed samples was very smooth, which are indicated by the surface roughness values below 1 nm (see Figure S1 in the Supporting Information).

The composition of CMD hydrogel layers was analyzed by XPS aiming to detect the presence of P atoms and thus determine the cross-linking degree. As only the STMP cross-linker molecules incorporated P atoms among the applied reagents, the detection of P could demonstrate the presence of cross-links. The analysis method we applied for the evaluation is detailed in the Supporting Information, and the resulting elemental composition of CMD samples can be seen in Figure S2. It was confirmed that the detected P signal in the completely rinsed sample originated from the P content of covalent cross-links, and the determined 0.2−0.4% P content corresponded to a cross-linking degree of around 5%.

The resulting CAs for both the aminosilane and CMD surfaces are shown in Figure 5. The advancing CA values of CMD surfaces were in the range of 10−30°. It was found that after water drop deposition, the drop shape remarkably varied in time. A typical result of the dynamic CA measurements can be seen in Figure 5A. The relaxation of CA was shown to be evident and, as a result of water absorption, the CA presented significant decrease as a function of measurement time. This

DOI: 10.1021/acs.langmuir.8b03249
Langmuir 2019, 35, 2412−2421

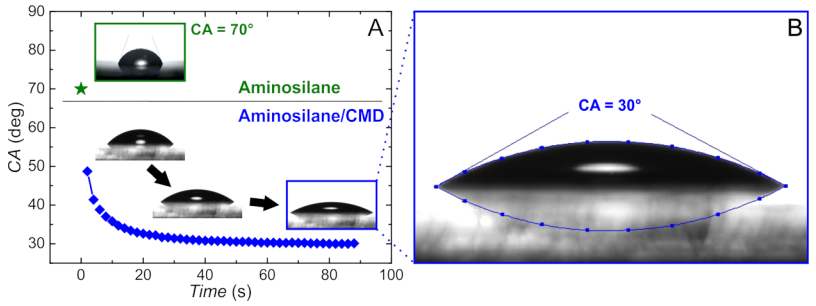

Figure 5. Water CAs on aminosilane and CMD surfaces. The top left inset image in A shows an aminosilylated sample (indicated by the green asterisk), and the images in the bottom half correspond to a spin-coated CMD sample (blue squares). Graph A shows the variation of CA as a function of time, representing the dynamic wetting properties of CMD hydrogel layers. B is an enlarged image from A, corresponding to the last measured point.

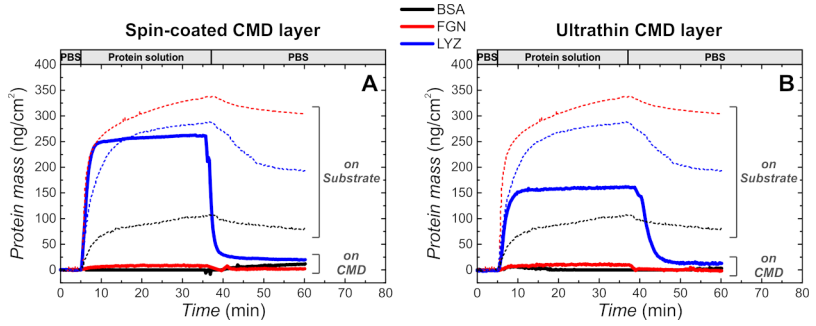

Figure 6. Adsorbed protein masses obtained from in situ OWLS-monitored NSB experiments on spin-coated (A) and ultrathin (B) CMD layers. The colors of curves represent the different proteins (BSA, FGN, and LYZ) used at 2 mg/mL concentration in the adsorption experiments. Whereas the solid lines indicate the data measured on CMD-covered surfaces, the dashed lines correspond to the data measured on the unmodified SiO_2−TiO_2 substrate surface.

observation demonstrates a typical characteristic of hydrogels verifying the hydrogel nature of the CMD layers.

3.1.2. Protein-Repellent Ability. The results of protein adsorption (NSB) tests performed on spin-coated (A) and ultrathin (B) CMD layers and monitored by the in situ OWLS technique are shown in Figure 6. The protein-repellent ability of the layers was evaluated by the amount (surface mass density) of proteins adsorbed. On the basis of the comparison of data measured on CMD surfaces with reference measurements, which were carried out on the unmodified SiO_2−TiO_2 substrate surface, it can be concluded that the CMD layer suppressed the adsorbed protein mass by about 1 order of magnitude. The slightly greater adsorbed mass values of LYZ are interpreted by the net positive charge of protein molecules (pI = 11.0), which resulted in higher attraction to the CMD chains (the pK_a value of CMD is around 3)[39] at the applied conditions (PBS medium, pH 7.4). Compared with the two types of CMD layers, the ultrathin coatings showed a slightly better NSB-resistant ability; however, the difference was not significant.

3.2. Results of Cell Micropatterning on CMD Surfaces. The CMD layers were printed with cRGDfK−AF patterns employing the FluidFM BOT setup to mediate cell adhesion by the patterns. The prints were examined by optical microscopy techniques. To receive a feedback about the printing and determine the pattern positions, the patterns had been checked in fluorescent mode before the samples were incubated with HeLa cells. After cell adhesion, phase contrast microscopy was applied to examine the adhered cells. Figure 7 presents two separate spot patterns indicated by SP1 and SP2, whereas Figure 8 shows three separate arrays of lines indicated

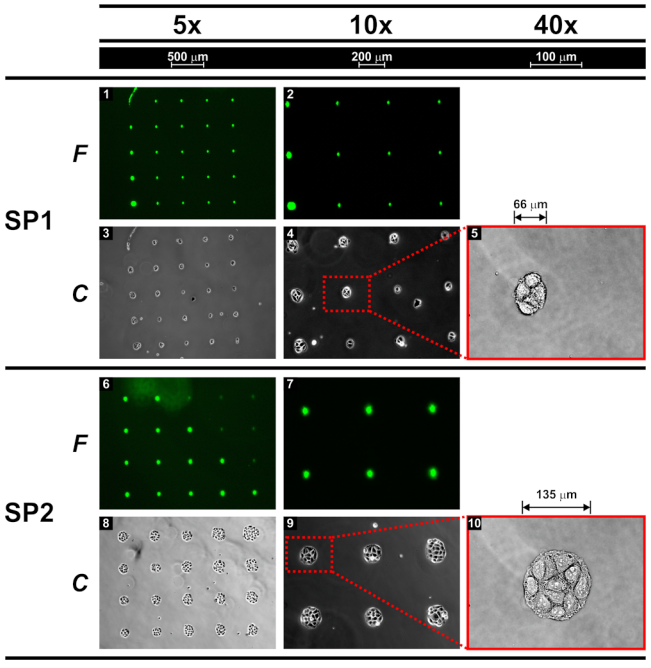

Figure 7. Fluorescent and phase contrast microscope images of two separate spot patterns (SP1 and SP2). The fluorescent images (row F) were captured before the incubation of samples in cell culture. After the adhesion of HeLa cells and subsequent fixation, the same patterns were captured by a phase contrast microscope (row C) in the same positions as used in the case of fluorescent images. The images were taken using 5×, 10×, and 40× objective lenses (as indicated by the header).

DOI: 10.1021/acs.langmuir.8b03249
Langmuir 2019, 35, 2412−2421

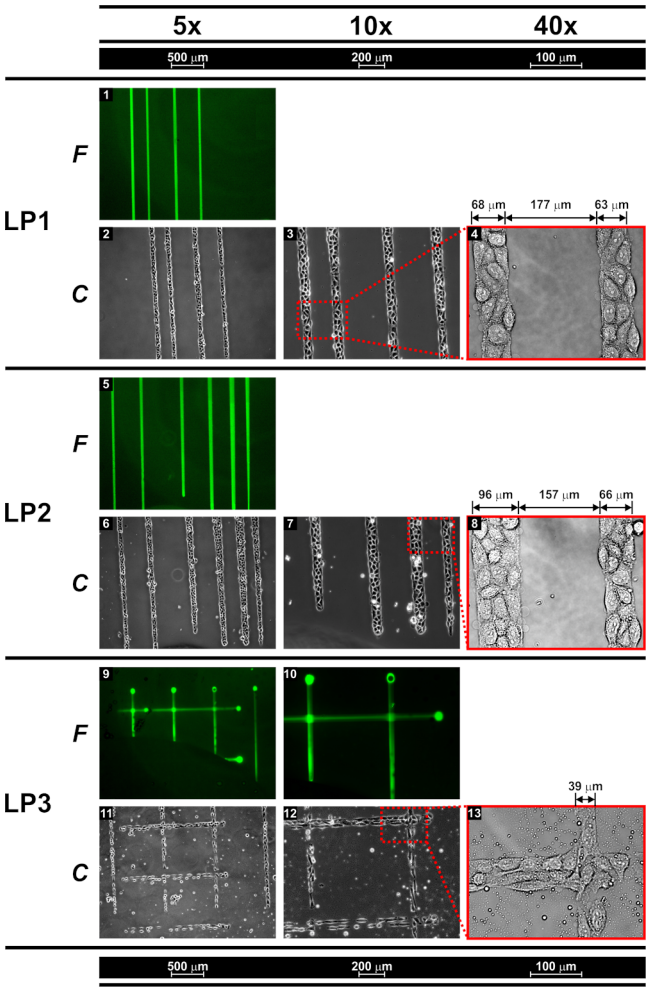

Figure 8. Fluorescent and phase contrast microscope images of three separate line patterns (LP1, LP2, and LP3). The fluorescent images (row F) were captured before the incubation of samples in cell culture. After the adhesion of HeLa cells and subsequent fixation, the same patterns were captured by a phase contrast microscope (row C) in the same positions as used in the case of fluorescent images (except LP3, at which the F and C images belong to similar but not to the same patterns). The images were taken using 5×, 10×, and 40× objective lenses (as indicated by the header). Note, in the case of images 11−13 (LP3), the small white dots are silicon oil contaminations that appeared during the cell fixation process because of the disassembly of the measurement chamber after the HoloMonitor experiment.

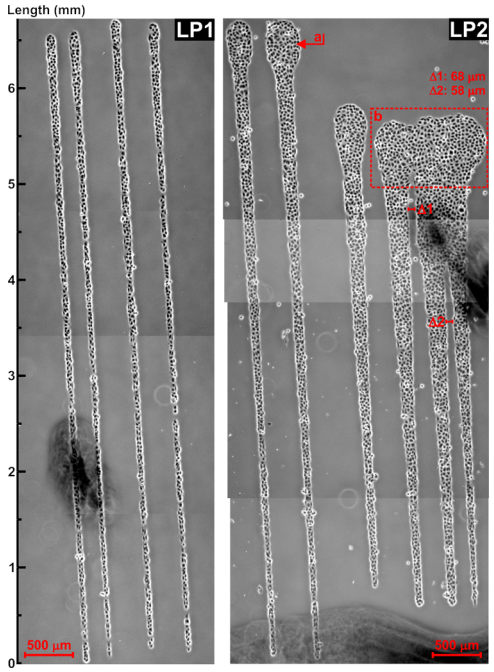

Figure 9. Phase contrast microscope images of two separate line patterns (LP1 and LP2), captured after the adhesion of HeLa cells on the cRGDfK-printed CMD surface. To have full images on the 5 and 6.5 mm long line patterns, 4−4 snapshots were merged to obtain the full-size images of LP1 and LP2. The blurry dark patches are caused by painted markers, which were used to facilitate the positioning of patterns. (a,b) Increased volume of printed cRGDfK−AF solution at the end of lines. (b) Fused lines of cells caused by the converged printed solution. (Δ1, Δ2) Line separation distances, demonstrating that the cells of the separate lines did not fuse when certain distances were reached (Δ1: 68 μm, Δ2: 58 μm).

by LP1, LP2, and LP3. The fluorescent and phase contrast images were captured in the same positions, providing effective comparison of the patterns before and after their incubation in cell culture. Images 1−4 (LP1) and 5−8 (LP2) in Figure 8 were captured on arrays of lines, which were printed with a maximal line length of 6.5 mm. To make these long lines visible, images from a large area were recorded and merged. Figure 9 presents two merged images of 4−4 smaller snapshots captured on the 6.5 mm long lines (LP1 and LP2). In these patterns, the cRGDfK−AF lines were printed with varying separation distances in order to investigate the minimum distance at which the lines of adhered cells remained separated and distinct. According to the observations, a distance of 60 μm was still enough for the separation (see Δ1 and Δ2 distances). As the LP2 b area of Figure 9 demonstrates, the cell patterns fused only when the cRGDfK patterns also merged supposedly caused by the convergence of the deposited solution patterns in the CMD layer.

As it can be seen in the images of Figure 9—especially in image LP2—wide oval-shaped cell area appeared at the certain ends of each line (indicated by a and b). These shapes were formed at the end of the line-printing process, when the micropipette was retracted to return to its starting position. During the retraction, some remaining solution leaked from the micropipette, increasing the deposited volume. The increased volume of the deposited solution is confirmed by the fluorescent images (Figure 8, images 9 and 10). The size of the area varied, and in effect, it depended on the actual condition of the micropipette, rather than the used printing parameters. The micropipette condition was sometimes disturbed by uncertain parameters, such as remaining solution and/or attached surface contaminations.

Figure 10 shows seven selected images from a time-lapse video that was recorded in situ using the DHM technique during the adhesion process. The results obtained from the combined FluidFM printing—cell adhesion experiments expressively proved the advantageous features of the developed CMD layers. The layer was amenable for the covalent attachment of cRGDfK motifs (easy-to-functionalize ability), it provided visible contrast between the printed and non-printed areas (cell-repellent vs biomimicking ability), and, modified with cRGDfK, it was an appropriate support for the adhered cells (ECM-like features). It is also worth highlighting that the cell adhesion experiments were performed in a serum-

DOI: 10.1021/acs.langmuir.8b03249
Langmuir 2019, 35, 2412−2421

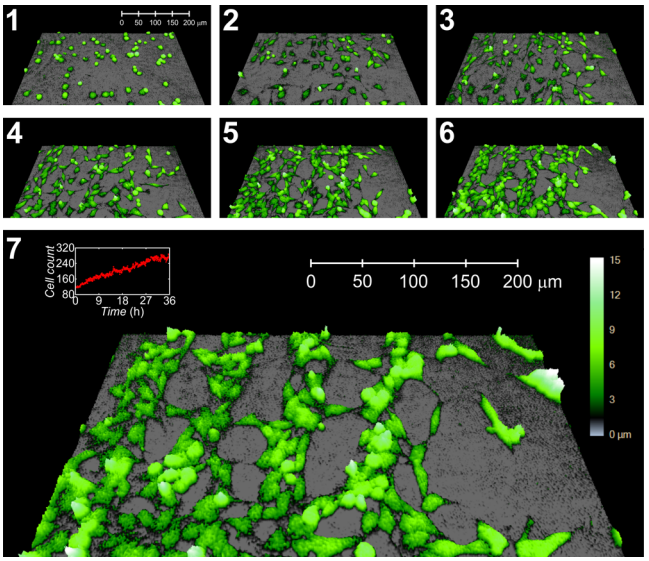

Figure 10. DHM images captured during the proceeding cell adhesion on the cRGDfK-printed CMD surface. The images were extracted from a time-lapse recording obtained by HoloMonitor M4. The images relate to the following incubation times: (1) 0 h (start), (2) 5, (3) 11.5, (4) 16, (5) 28.5, (6) 33 h, and (7) 36 h (end). The inset graph of image 7 represents the increasing number of proliferating cells (cell count) during the observation time. Note the field view was fixed at 558 × 558 μm, limiting the complete observation of the millimeter long lines.

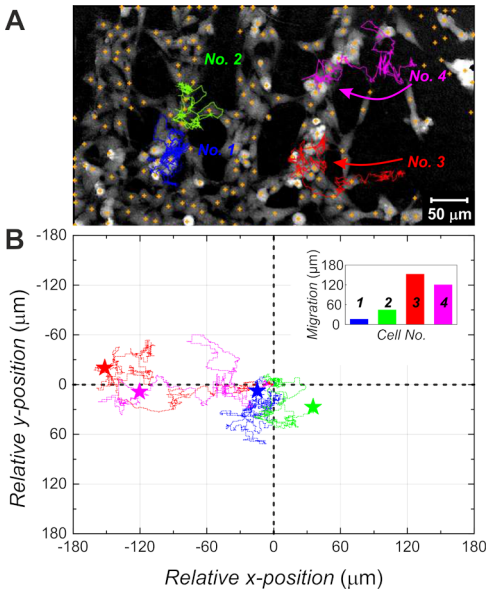

Figure 11. Tracking the migration of four individual cells using HoloMonitor M4. (A) Holographic microscope image captured at the 36th hour of incubation. The paths migrated by the tracked cells from their initial position are indicated by colored lines. While the initial position of cell nos. 1 and 2 was on a printed cRGDfK line, cell nos. 3 and 4 started their migration from a cRGDfK-free area (see the arrows indicating the direction of migration). (B) Graph representing the positions and migrated path of the tracked cells relative to their initial position (coordinate (0,0)). The colored stars indicate the final position of the cells. The inset graph of plot B shows the linear distance between the initial and the end position of the tracked cells.

containing medium. Serum proteins adsorbed on a surface could easily turn an originally cell-repellent layer to highly cell-adhesive. Consequently, if the adsorption of the proteins had occurred, cell adhesion should have been observed. As a result, the strong cell-repellent ability (as verified by the cell adhesion experiments) was an indirect proof of the protein-repellent ability of the CMD layer.

The behavior of cells on the printed line arrays was quantified using data obtained from DHM measurements. The increasing number of cells in the inset graph of image 7 (Figure 10) shows that the cells could proliferate on the cRGDfK-functionalized lines.

To characterize the migration abilities, four individual cells were selected on the captured DHM images and tracked throughout the applied incubation time (36 h) (see Figure 11A). As indicated by the colored lines representing the migrated path of the tracked cells, while cell nos. 1 and 2 migrated around a relatively small area, the linear distance between the end and initial position of cell nos. 3 and 4 was several times greater [on average 31 μm (nos. 1 and 2) versus 137 μm (nos. 3 and 4), respectively]. This observation was due to the fact that while the initial position of cell nos. 1 and 2 was on a cRGDfK line, cell nos. 3 and 4 were on a cRGDfK-free area, forcing them to migrate onto the closest area functionalized with cRGDfK motifs. The migrated path of the tracked cells relative to their initial position can be seen in graph B of Figure 11. Herein, the inset graph represents the migrated linear distance of cells measured between their initial and final positions.

4. SUMMARY AND CONCLUSIONS

In this study, we have presented the development of cell micropatterns on CMD-based hydrogel surfaces using the FluidFM BOT technology. We have shown that the new type of chemically cross-linked CMD hydrogel layers provided suitable support for FluidFM-based cell patterning experiments demonstrating their potential applications in cell-on-a-chip or tissue-on-a-chip biosensors. The presence of covalent cross-links in the hydrogel layers was verified (cross-linking degree: 5%), and the thickness of the stable CMD layers was determined to be in the range of 10−50 nm. The protein-repellent ability was verified by in situ OWLS measurements. It was shown that the CMD layer suppressed the adsorption of serum proteins by 1 order of magnitude compared to the unmodified SiO_2−TiO_2 reference surfaces.

Exploiting the advantageous properties of the developed CMD hydrogel layers, cell adhesion mediating cRGDfK molecules were printed onto CMD surfaces by the FluidFM BOT technology. The adhesion of living cells on the patterns was monitored by phase contrast microscopy and DHM. The analysis of DHM images revealed that the cells, initially deposited on a cRGDfK-printed line, showed random migration around their initial position. In contrast, other cells with initial positions distant from cRGDfK lines migrated along a specific direction until reaching the closest cRGDfK-covered area.

We demonstrated that the FluidFM can be efficiently used for printing micro-scale patterns of biomolecules on large millimeter−centimeter-scale surface areas in various pattern geometries. The printing was performed directly from liquid phase with few minutes of processing time. These unique features of bioprinting technology are of high importance in the field of single-cell analysis and manipulation. The significance can be found in the case of those plate-based biochemical assays and biosensors, where the ability to perform

DOI: 10.1021/acs.langmuir.8b03249
Langmuir 2019, 35, 2412−2421

fast, versatile, automated, and large-scale surface modifications is crucial.

Because of the possibility of printing micron-scale cellular patterns on millimeter- and centimeter-scale areas, the developed methodologies are especially suitable for high-throughput screening applications in combination with novel biosensor technologies.[40−43]

■ ASSOCIATED CONTENT

Supporting Information

The Supporting Information is available free of charge on the ACS Publications website at DOI: 10.1021/acs.langmuir.8b03249.

Parameter settings in FluidFM printing experiments, AFM topographic images of CMD surfaces, elemental composition of the CMD layers, and additional details about the CMD layers' wetting behavior (PDF)

■ AUTHOR INFORMATION

Corresponding Author

*E-mail: saftics.andras@energia.mta.hu. Phone: 003613922696.

ORCID

Andras Saftics: 0000-0001-7129-6142

Robert Horvath: 0000-0001-8617-2302

Notes

The authors declare no competing financial interest.

■ ACKNOWLEDGMENTS

The present work was funded by the Momentum Program ("Lendület") of the Hungarian Academy of Sciences as well as by the ERC-HU Program, the KH-17, and FK-128901 project of NKFIH. Support from the János Bolyai Research Scholarship of the Hungarian Academy of Sciences (S.K.) is also gratefully acknowledged.

■ REFERENCES

(1) Wang, J.-C.; Liu, W.; Tu, Q.; Ma, C.; Zhao, L.; Wang, Y.; Ouyang, J.; Pang, L.; Wang, J. High Throughput and Multiplex Localization of Proteins and Cells for in Situ Micropatterning Using Pneumatic Microfluidics. *Analyst* **2015**, *140*, 827−836.

(2) El-Ali, J.; Sorger, P. K.; Jensen, K. F. Cells on Chips. *Nature* **2006**, *442*, 403−411.

(3) Seliktar, D. Designing Cell-Compatible Hydrogels for Biomedical Applications. *Science* **2012**, *336*, 1124−1128.

(4) Nath, N.; Hyun, J.; Ma, H.; Chilkoti, A. Surface Engineering Strategies for Control of Protein and Cell Interactions. *Surf. Sci.* **2004**, *570*, 98−110.

(5) Zhang, Y. S.; Khademhosseini, A. Advances in Engineering Hydrogels. *Science* **2017**, *356*, No. eaaf3627.

(6) Löfås, S.; Johnsson, B. A Novel Hydrogel Matrix on Gold Surfaces in Surface Plasmon Resonance Sensors for Fast and Efficient Covalent Immobilization of Ligands. *J. Chem. Soc., Chem. Commun.* **1990**, *21*, 1526−1528.

(7) McArthur, S. L.; McLean, K. M.; Kingshott, P.; St John, H. A. W.; Chatelier, R. C.; Griesser, H. J. Effect of Polysaccharide Structure on Protein Adsorption. *Colloids Surf., B* **2000**, *17*, 37−48.

(8) Monchaux, E.; Vermette, P. Cell Adhesion Resistance Mechanisms Using Arrays of Dextran-Derivative Layers. *J. Biomed. Mater. Res., Part A* **2008**, *85*, 1052−1063.

(9) Lee, M. H.; Boettiger, D.; Composto, R. J. Biomimetic Carbohydrate Substrates of Tunable Properties Using Immobilized Dextran Hydrogels. *Biomacromolecules* **2008**, *9*, 2315−2321.

(10) Saftics, A.; Kurunczi, S.; Szekrényes, Z.; Kamarás, K.; Khánh, N. Q.; Sulyok, A.; Bssze, S.; Horvath, R. Fabrication and Characterization of Ultrathin Dextran Layers: Time Dependent Nanostructure in Aqueous Environments Revealed by OWLS. *Colloids Surf., B* **2016**, *146*, 861−870.

(11) Saftics, A.; Prósz, G. A.; Türk, B.; Peter, B.; Kurunczi, S.; Horvath, R. In Situ Viscoelastic Properties and Chain Conformations of Heavily Hydrated Carboxymethyl Dextran Layers: A Comparative Study Using OWLS and QCM-I Chips Coated with Waveguide Material. *Sci. Rep.* **2018**, *8*, 11840.

(12) Saftics, A.; Kurunczi, S.; Türk, B.; Agócs, E.; Kalas, B.; Petrik, P.; Fried, M.; Sulyok, A.; Bősze, S.; Horvath, R. Spin Coated Carboxymethyl Dextran Layers on TiO2-SiO2 Optical Waveguide Surfaces. *Rev. Roum. Chim.* **2017**, *62*, 775−781.

(13) Lodish, H.; Berk, A.; Matsudaira, P.; Kaiser, C. A.; Krieger, M.; Scott, M. P.; Zipursky, L.; Darnell, J. *Molecular Cell Biology*, 5th ed.; W. H. Freeman & Co., 2003.

(14) Lévesque, S. G.; Shoichet, M. S. Synthesis of Cell-Adhesive Dextran Hydrogels and Macroporous Scaffolds. *Biomaterials* **2006**, *27*, 5277−5285.

(15) Riahi, N.; Liberelle, B.; Henry, O.; De Crescenzo, G. Impact of RGD Amount in Dextran-Based Hydrogels for Cell Delivery. *Carbohydr. Polym.* **2017**, *161*, 219−227.

(16) Hadjizadeh, A.; Doillon, C. J.; Vermette, P. Bioactive Polymer Fibers to Direct Endothelial Cell Growth in a Three-Dimensional Environment. *Biomacromolecules* **2007**, *8*, 864−873.

(17) Massia, S. P.; Stark, J.; Letbetter, D. S. Surface-Immobilized Dextran Limits Cell Adhesion and Spreading. *Biomaterials* **2000**, *21*, 2253−2261.

(18) Massia, S. P.; Stark, J. Immobilized RGD Peptides on Surface-Grafted Dextran Promote Biospecific Cell Attachment. *J. Biomed. Mater. Res.* **2001**, *56*, 390−399.

(19) Danhier, F.; Le Breton, A.; Préat, V. RGD-Based Strategies to Target Alpha(v) Beta(3) Integrin in Cancer Therapy and Diagnosis. *Mol. Pharm.* **2012**, *9*, 2961−2973.

(20) Ruoslahti, E. RGD and Other Recognition Sequences for Integrins. *Annu. Rev. Cell Dev. Biol.* **1996**, *12*, 697−715.

(21) Liu, W.-W.; Chen, Z.-L.; Jiang, X.-Y. Methods for Cell Micropatterning on Two-Dimensional Surfaces and Their Applications in Biology. *Chin. J. Anal. Chem.* **2009**, *37*, 943−949.

(22) Yousaf, M. N.; Houseman, B. T.; Mrksich, M. Using electroactive substrates to pattern the attachment of two different cell populations. *Proc. Natl. Acad. Sci. U.S.A.* **2001**, *98*, 5992−5996.

(23) Mrksich, M. A surface chemistry approach to studying cell adhesion. *Chem. Soc. Rev.* **2000**, *29*, 267−273.

(24) Wang, X.; Li, S.; Yan, C.; Liu, P.; Ding, J. Fabrication of RGD Micro/Nanopattern and Corresponding Study of Stem Cell Differentiation. *Nano Lett.* **2015**, *15*, 1457−1467.

(25) Yan, C.; Sun, J.; Ding, J. Critical areas of cell adhesion on micropatterned surfaces. *Biomaterials* **2011**, *32*, 3931−3938.

(26) Salaita, K.; Wang, Y.; Mirkin, C. A. Applications of Dip-Pen Nanolithography. *Nat. Nanotechnol.* **2007**, *2*, 145−155.

(27) Meister, A.; Gabi, M.; Behr, P.; Studer, P.; Vörös, J.; Niedermann, P.; Bitterli, J.; Polesel-Maris, J.; Liley, M.; Heinzelmann, H.; et al. FluidFM: Combining Atomic Force Microscopy and Nanofluidics in a Universal Liquid Delivery System for Single Cell Applications and Beyond. *Nano Lett.* **2009**, *9*, 2501−2507.

(28) Grüter, R. R.; Vörös, J.; Zambelli, T. FluidFM as a Lithography Tool in Liquid: Spatially Controlled Deposition of Fluorescent Nanoparticles. *Nanoscale* **2013**, *5*, 1097−1104.

(29) Hirt, L.; Ihle, S.; Pan, Z.; Dorwling-Carter, L.; Reiser, A.; Wheeler, J. M.; Spolenak, R.; Vörös, J.; Zambelli, T. Template-Free 3D Microprinting of Metals Using a Force-Controlled Nanopipette for Layer-by-Layer Electrodeposition. *Adv. Mater.* **2016**, *28*, 2311−2315.

(30) Ventrici de Souza, J.; Liu, Y.; Wang, S.; Dörig, P.; Kuhl, T. L.; Frommer, J.; Liu, G.-y. Three-Dimensional Nanoprinting via Direct Delivery. *J. Phys. Chem. B* **2017**, *122*, 956−962.

DOI: 10.1021/acs.langmuir.8b03249
Langmuir 2019, 35, 2412−2421

(31) Meister, A.; Polesel-Maris, J.; Niedermann, P.; Przybylska, J.; Studer, P.; Gabi, M.; Behr, P.; Zambelli, T.; Liley, M.; Vörös, J.; et al. Nanoscale Dispensing in Liquid Environment of Streptavidin on a Biotin-Functionalized Surface Using Hollow Atomic Force Microscopy Probes. *Microelectron. Eng.* **2009**, *86*, 1481−1484.
(32) Huynh, R.; Chaubet, F.; Jozefonvicz, J. Carboxymethylation of Dextran in Aqueous Alcohol as the First Step of the Preparation of Derivatized Dextrans. *Angew Makromol. Chem.* **1998**, *254*, 61−65.
(33) Gao, F.; Li, D.; Bi, C.-h.; Mao, Z.-h.; Adhikari, B. Preparation and Characterization of Starch Crosslinked with Sodium Trimetaphosphate and Hydrolyzed by Enzymes. *Carbohydr. Polym.* **2014**, *103*, 310−318.
(34) Seker, M.; Hanna, M. A. Sodium Hydroxide and Trimetaphosphate Levels Affect Properties of Starch Extrudates. *Ind. Crops Prod.* **2006**, *23*, 249−255.
(35) Wintgens, V.; Lorthioir, C.; Dubot, P.; Sébille, B.; Amiel, C. Cyclodextrin/Dextran Based Hydrogels Prepared by Cross-Linking with Sodium Trimetaphosphate. *Carbohydr. Polym.* **2015**, *132*, 80−88.
(36) Stalder, A. F.; Kulik, G.; Sage, D.; Barbieri, L.; Hoffmann, P. A Snake-Based Approach to Accurate Determination of Both Contact Points and Contact Angles. *Colloids Surf., A* **2006**, *286*, 92−103.
(37) Guillaume-Gentil, O.; Potthoff, E.; Ossola, D.; Franz, C. M.; Zambelli, T.; Vorholt, J. A. Force-Controlled Manipulation of Single Cells: From AFM to FluidFM. *Trends Biotechnol.* **2014**, *32*, 381−388.
(38) Peter, B.; Nador, J.; Juhasz, K.; Dobos, A.; Korosi, L.; Székács, I.; Patko, D.; Horvath, R. Incubator proof miniaturized Holomonitor toin situmonitor cancer cells exposed to green tea polyphenol and preosteoblast cells adhering on nanostructured titanate surfaces: validity of the measured parameters and their corrections. *J. Biomed. Opt.* **2015**, *20*, 067002.
(39) Sidobre, S.; Puzo, G.; Rivière, M. Lipid-Restricted Recognition of Mycobacterial Lipoglycans by Human Pulmonary Surfactant Protein A: A Surface-Plasmon-Resonance Study. *Biochem. J.* **2002**, *365*, 89−97.
(40) Orgovan, N.; Peter, B.; Bősze, S.; Ramsden, J. J.; Szabó, B.; Horvath, R. Dependence of Cancer Cell Adhesion Kinetics on Integrin Ligand Surface Density Measured by a High-Throughput Label-Free Resonant Waveguide Grating Biosensor. *Sci. Rep.* **2014**, *4*, 4034.
(41) Peter, B.; Farkas, E.; Forgacs, E.; Saftics, A.; Kovacs, B.; Kurunczi, S.; Szekacs, I.; Csampai, A.; Bosze, S.; Horvath, R. Green Tea Polyphenol Tailors Cell Adhesivity of RGD Displaying Surfaces: Multicomponent Models Monitored Optically. *Sci. Rep.* **2017**, *7*, 42220.
(42) Farkas, E.; Szekacs, A.; Kovacs, B.; Olah, M.; Horvath, R.; Szekacs, I. Label-Free Optical Biosensor for Real-Time Monitoring the Cytotoxicity of Xenobiotics: A Proof of Principle Study on Glyphosate. *J. Hazard. Mater.* **2018**, *351*, 80−89.
(43) Peter, B.; Lagzi, I.; Teraji, S.; Nakanishi, H.; Cervenak, L.; Zámbó, D.; Deák, A.; Molnár, K.; Truszka, M.; Szekacs, I.; et al. Interaction of Positively Charged Gold Nanoparticles with Cancer Cells Monitored by an in Situ Label-Free Optical Biosensor and Transmission Electron Microscopy. *ACS Appl. Mater. Interfaces* **2018**, *10*, 26841−26850.

DOI: 10.1021/acs.langmuir.8b03249
Langmuir 2019, 35, 2412−2421